

Supplementary Material

Novel high-entropy sulfide (ZnCoMnFeAlMg)₉S₈ as low potential and long life electrocatalyst for overall water splitting in experiments and DFT analysis

Shun Li^a, Likai Tong^a, Zhijian Peng^b, Bo Zhang^a and Xiuli Fu^{a,*}

^a School of Integrated Circuits, Beijing University of Posts and Telecommunications, Beijing

100876, P. R. China

^b School of Science, China University of Geosciences, Beijing 100083, P. R. China

Corresponding authors

* Telephone: 86-10-62282452. Fax: 86-10-62282054

E-mail: xiulifu@bupt.edu.cn (X. Fu)

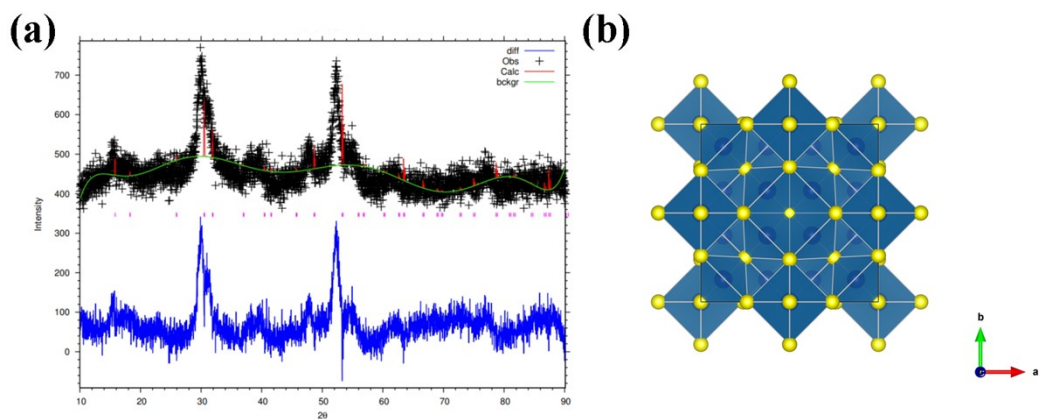


Fig. S1 (a) The refined XRD pattern and (b) schematic representation of the crystal structure for $(\text{ZnCoMnFeAlMg})_9\text{S}_8$.

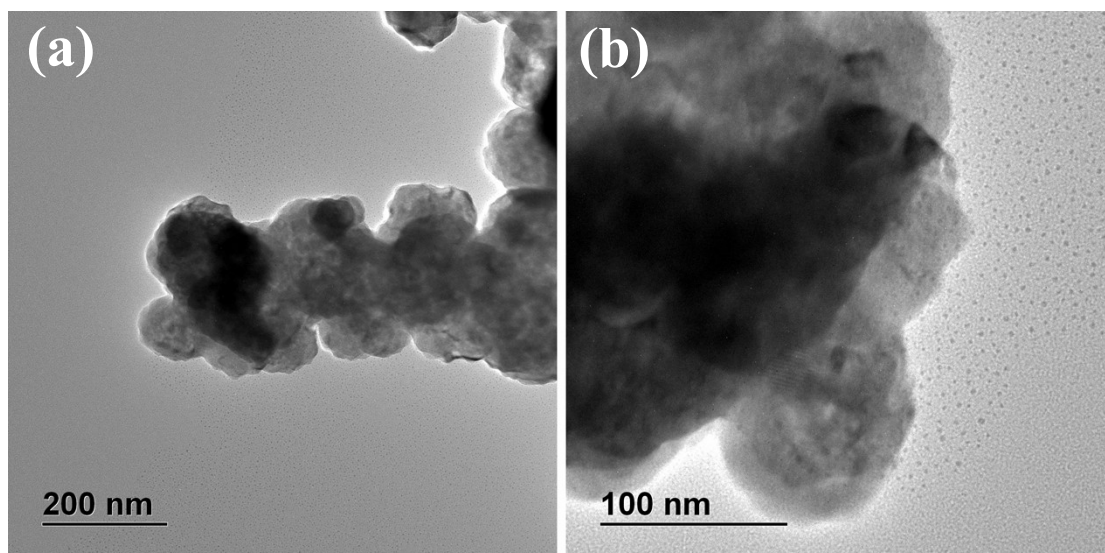


Fig. S2 Different magnification TEM images of $(\text{ZnCoMnFeAlMg})_9\text{S}_8$.

It is obvious that the structure of $(\text{ZnCoMnFeAlMg})_9\text{S}_8$ is nanoscale fragments.

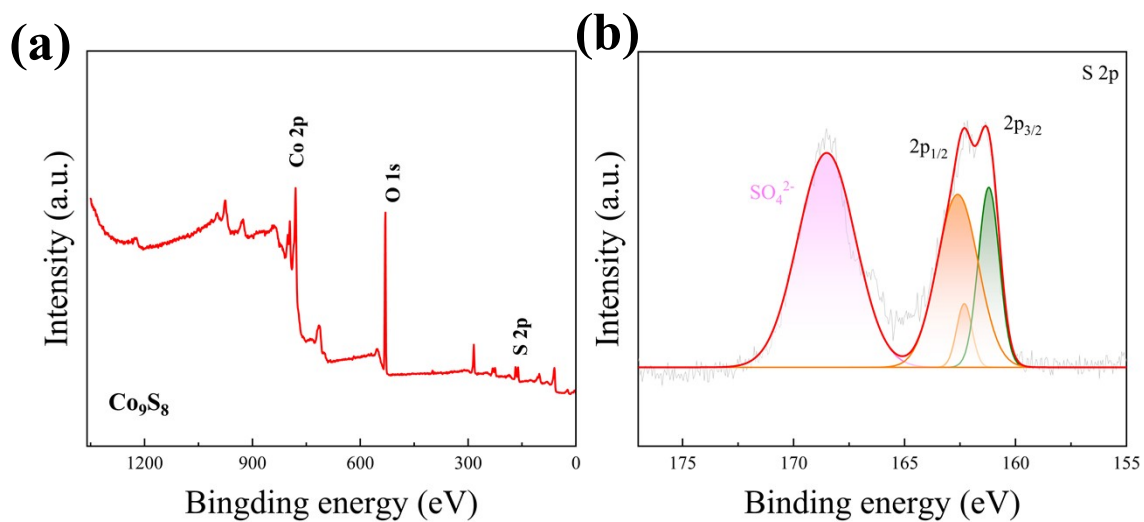


Fig. S3 XPS data of Co_9S_8 . (a) XPS survey spectrum and (b) S 2p.

In brief, the spectrum indicates the presence of cobalt (Co 2p), sulfur (S 2p), and oxygen (O 1s). The S 2p spectrum of Co_9S_8 shown in Fig. S2(b) indicates the dominance of S^{2-} and bridging S_2^{2-} species, confirming the formation of Co_9S_8 . Besides, a small amount of SO_4^{2-} ions can be detected, which combines with multivalent metal species to enhance the overall water splitting performance

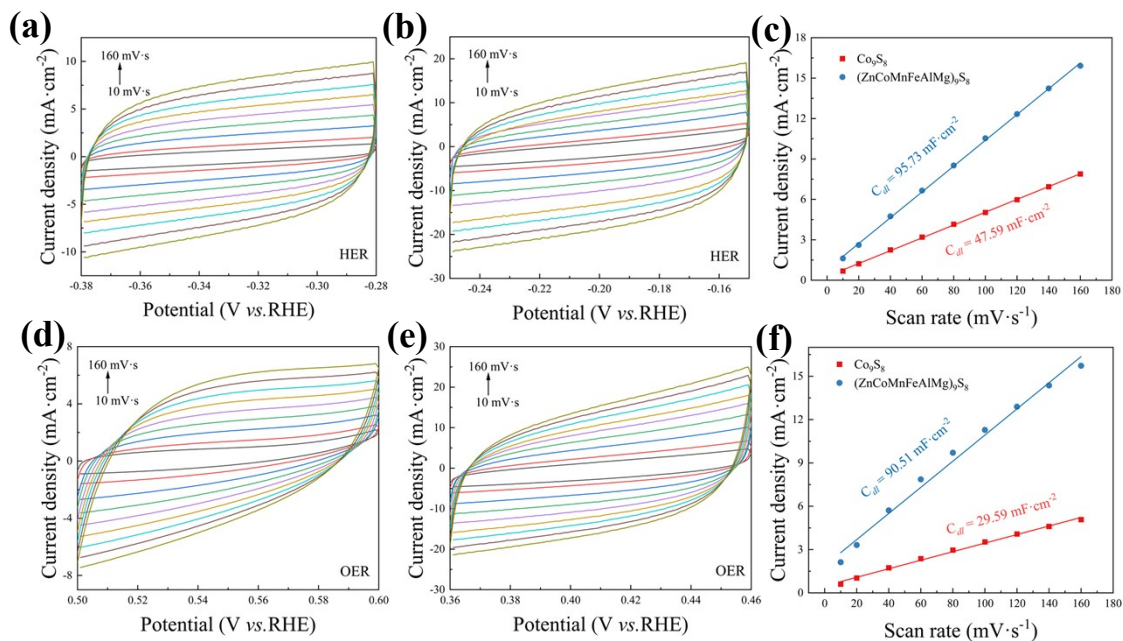


Fig. S4 Cyclic voltammograms of (a,d) Co_9S_8 , and (b,e) $(\text{ZnCoMnFeAlMg})_9\text{S}_8$. Capacitance current as a function of scan rates (c) Co_9S_8 , (f) $(\text{ZnCoMnFeAlMg})_9\text{S}_8$.

In order to obtain ECSA, CV tests were conducted on Co_9S_8 and $(\text{ZnCoMnFeAlMg})_9\text{S}_8$ at 10–160 mV s^{-1} . The results show that for both the HER process and the OER process, the fitted C_{dl} values of $(\text{ZnCoMnFeAlMg})_9\text{S}_8$ are higher than those of Co_9S_8 .

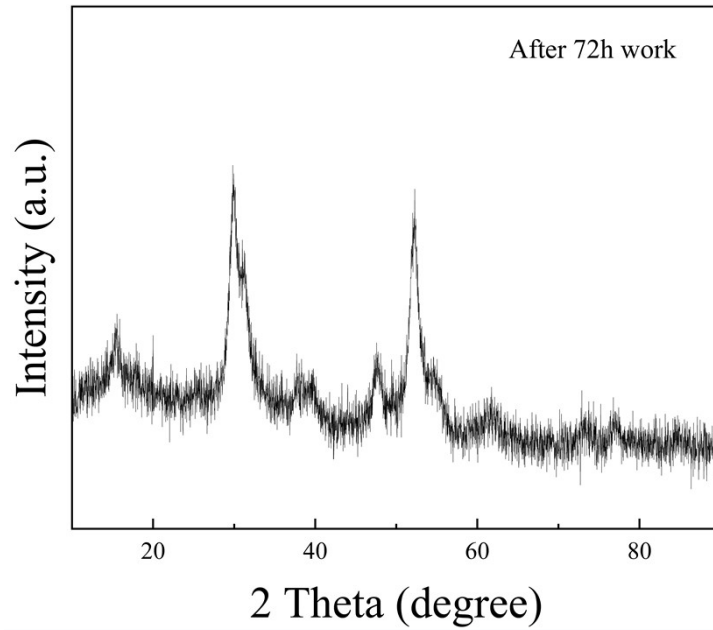


Fig. S5 XRD pattern of the $(\text{ZnCoMnFeAlMg})_9\text{S}_8$ after 72 h work.

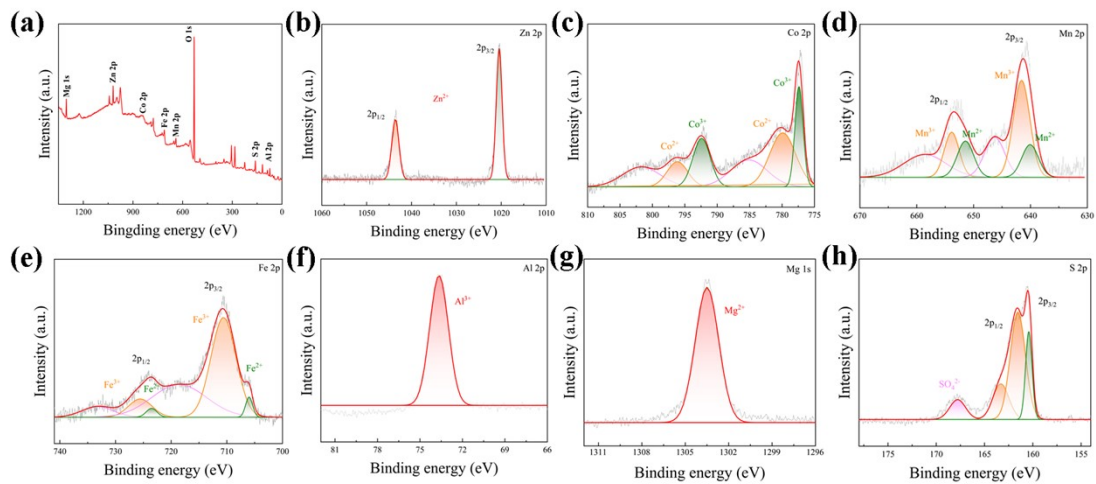


Fig. S6 XPS data of $(\text{ZnCoMnFeAlMg})_9\text{S}_8$ after 72 h work. (a) survey spectrum and high-resolution spectra of (b) Zn 2p, (c) Co 2p, (d) Mn 2p, (e) Fe 2p, (f) Al 2p, (g) Mg 1s, and (h) S 2p.

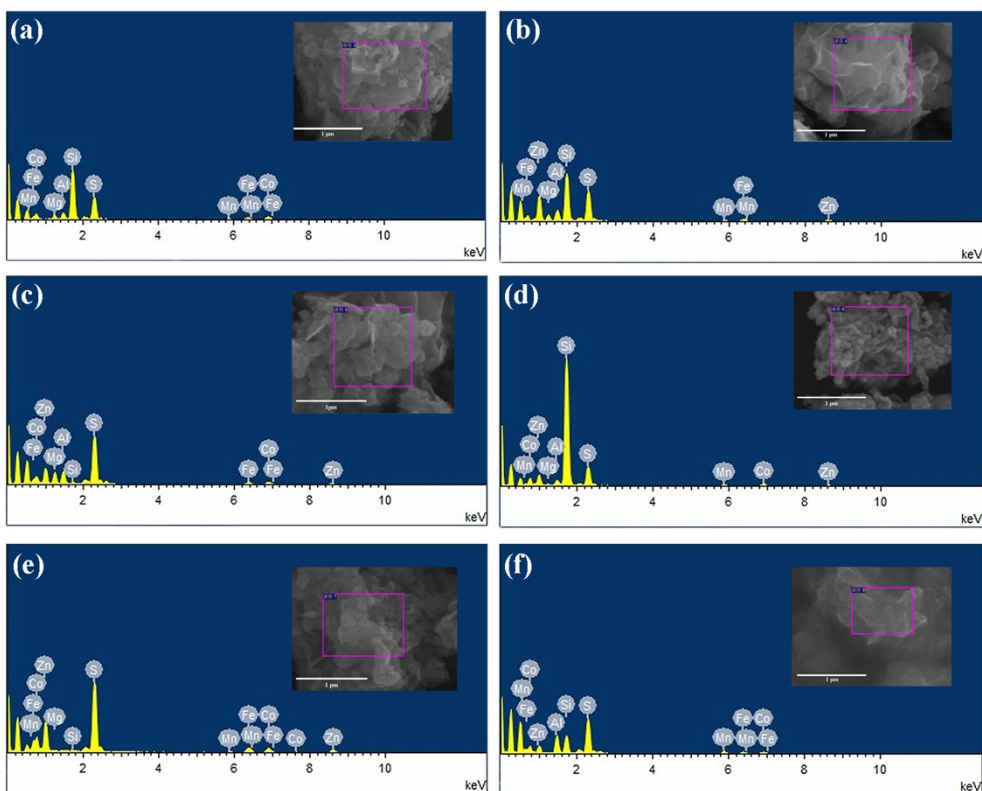


Fig. S7 The EDS results after removing one metal element from $(\text{ZnCoMnFeAlMg})_9\text{S}_8$ are presented. (a) $(\text{CoMnFeAlMg})_9\text{S}_8$, (b) $(\text{ZnMnFeAlMg})_9\text{S}_8$, (c) $(\text{ZnCoFeAlMg})_9\text{S}_8$, (d) $(\text{ZnCoMnAlMg})_9\text{S}_8$, (e) $(\text{ZnCoMnFeMg})_9\text{S}_8$, and (f) $(\text{ZnCoMnFeAl})_9\text{S}_8$.

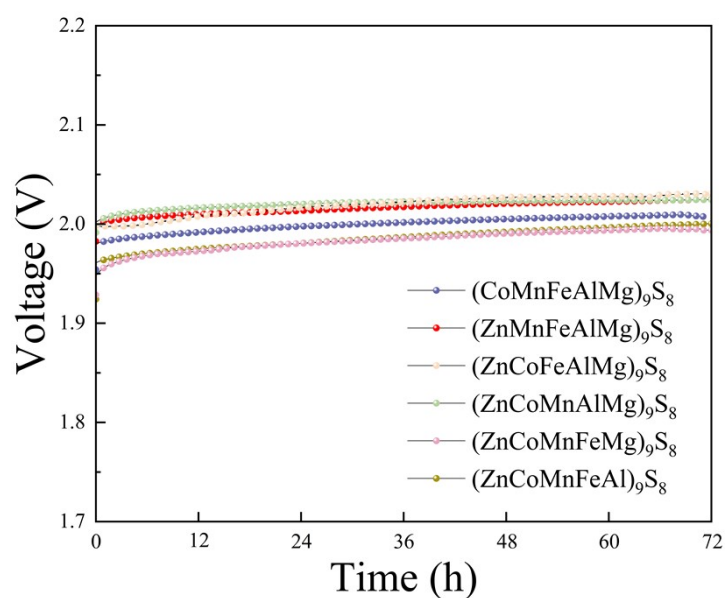


Fig. S8 Comparison of the working stability and overpotential among different catalysts.

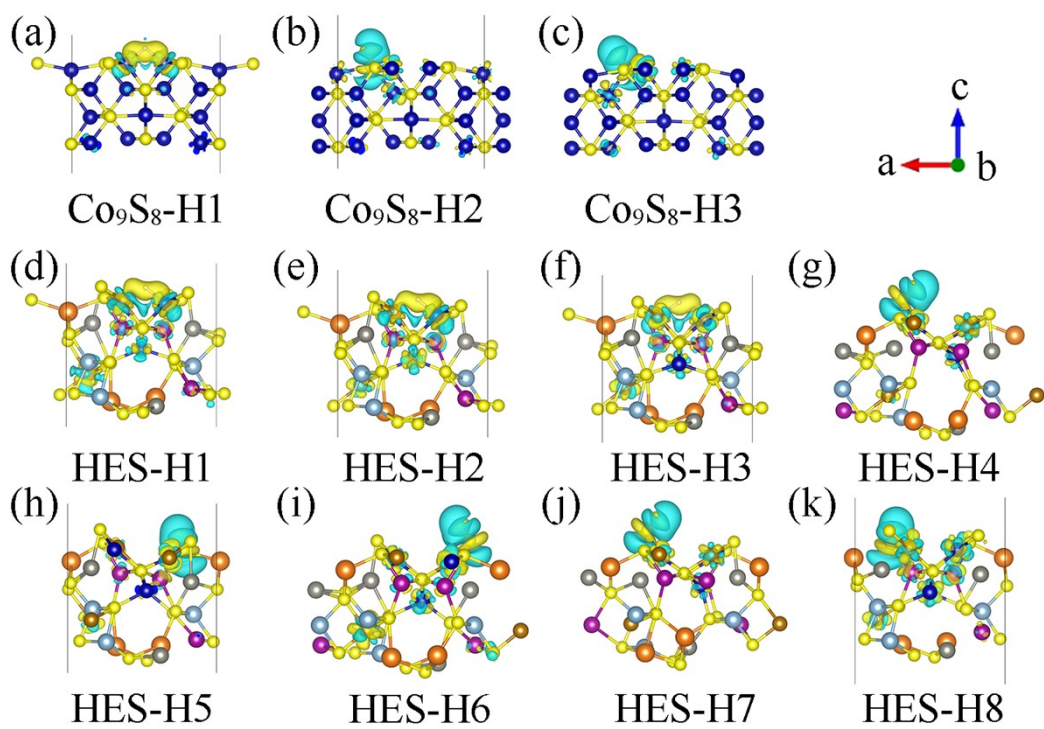


Fig. S9 Charge density difference for the H^* adsorbed on (a-c) Co_9S_8 and (d-k) $(\text{ZnCoMnFeAlMg})_9\text{S}_8$

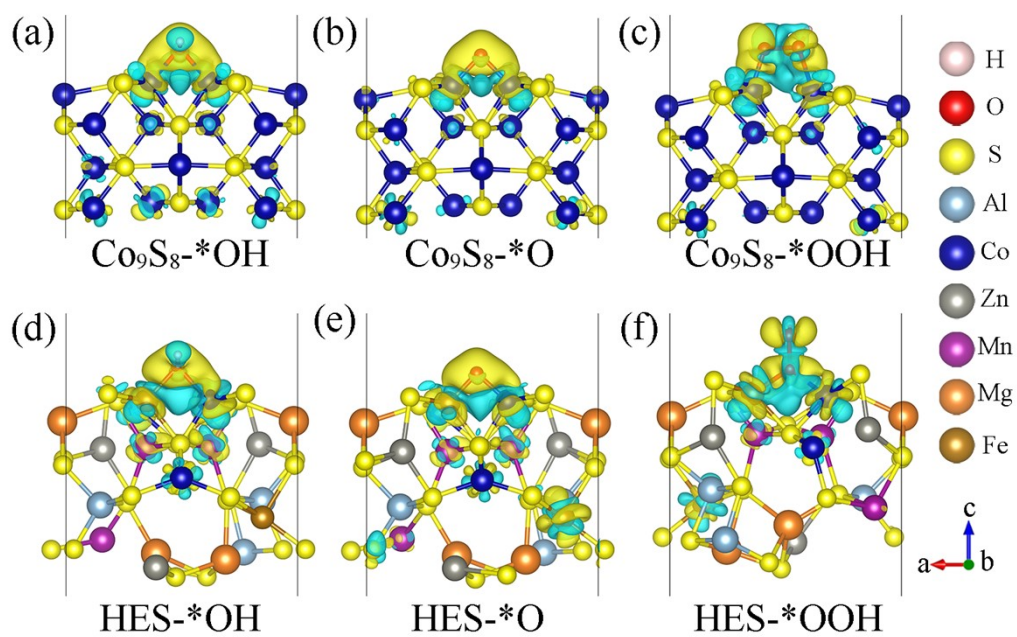


Fig. S10 Charge density difference for the OOH^* adsorbed on (a-c) Co_9S_8 and (d-f) $(\text{ZnCoMnFeAlMg})_9\text{S}_8$

Table. S1. The atomic positions in the obtained HES structure are as follows.

	x	y	z		x	y	z
M1	0.12641	0.12641	0.12641	S1	0	0	0.26121
M2	0.87359	0.87359	0.87359	S2	0	0	0.73879
M3	0.87359	0.87359	0.12641	S3	0.26121	0	0
M4	0.12641	0.12641	0.87359	S4	0.73879	0	0
M5	0.87359	0.12641	0.87359	S5	0	0.26121	0
M6	0.12641	0.87359	0.12641	S6	0	0.73879	0
M7	0.12641	0.87359	0.87359	S7	0	0.5	0.76121
M8	0.87359	0.12641	0.12641	S8	0	0.5	0.23879
M9	0.12641	0.62641	0.62641	S9	0.26121	0.5	0.5
M10	0.87359	0.37359	0.37359	S10	0.73879	0.5	0.5
M11	0.87359	0.37359	0.62641	S11	0	0.76121	0.5
M12	0.12641	0.62641	0.37359	S12	0	0.23879	0.5
M13	0.87359	0.62641	0.37359	S13	0.5	0	0.76121
M14	0.12641	0.37359	0.62641	S14	0.5	0	0.23879
M15	0.12641	0.37359	0.37359	S15	0.76121	0	0.5
M16	0.87359	0.62641	0.62641	S16	0.23879	0	0.5
M17	0.62641	0.12641	0.62641	S17	0.5	0.26121	0.5
M18	0.37359	0.87359	0.37359	S18	0.5	0.73879	0.5
M19	0.37359	0.87359	0.62641	S19	0.5	0.5	0.26121
M20	0.62641	0.12641	0.37359	S20	0.5	0.5	0.73879
M21	0.37359	0.12641	0.37359	S21	0.76121	0.5	0
M22	0.62641	0.87359	0.62641	S22	0.23879	0.5	0
M23	0.62641	0.87359	0.37359	S23	0.5	0.76121	0
M24	0.37359	0.12641	0.62641	S24	0.5	0.23879	0
M25	0.62641	0.62641	0.12641	S25	0.25	0.25	0.25
M26	0.37359	0.37359	0.87359	S26	0.75	0.75	0.75
M27	0.37359	0.37359	0.12641	S27	0.75	0.75	0.25
M28	0.62641	0.62641	0.87359	S28	0.25	0.25	0.75
M29	0.37359	0.62641	0.87359	S29	0.75	0.25	0.75
M30	0.62641	0.37359	0.12641	S30	0.25	0.75	0.25
M31	0.62641	0.37359	0.87359	S31	0.25	0.75	0.75
M32	0.37359	0.62641	0.12641	S32	0.75	0.25	0.25
M33	0	0	0.5				
M34	0.5	0	0				
M35	0	0.5	0				
M36	0.5	0.5	0.5				

Table. S2 Sulfide-based dual-functional electrocatalysts and other commercial electrocatalysts for overall water splitting.

Electrocatalyst	HER	OER	Overall	Stability	Ref.
	[mV@mA cm ⁻²]	[mV@mA cm ⁻²]	[V@mA cm ⁻²]		
Co ₉ S ₈ @Ni(OH) ₂	100@10	250@60	1.55@10	10 h	[35]
CoS–Co(OH) ₂ @MoS _{2+x}	143@10	380@10	1.58@10	11 h	[6]
Co ₃ S ₄ @MoS ₂	136@10	280@20	1.58@10	10 h	[36]
(Ni, Fe)S ₂ @MoS ₂	130@10	270@10	1.56@10	45 h	[37]
Se–MnS/NiS	56@10	211@10	1.47@10	48 h	[38]
V–Ni ₃ S ₂	133@10	148@10	1.42@10	60 h	[39]
N-CNTs/NiS ₂ @Mo ₂ C	227@10	320@10	1.52@10	24 h	[40]
N-Ni ₃ S ₂ /VS ₂	151@10	227@10	1.65@10	20 h	[41]
Pt/C/NF//RuO ₂ /NF			1.71@10		[42]
RuO ₂ /NF		290@10			[43]
Pt/C/NF	30@10				[43]
(ZnCoMnFeAlMg) ₉ S ₈ /NF	160@10	170@10	1.39@10	72 h	This work

Table. S3 Statistical table of Co_9S_8 adsorption sites and corresponding Gibbs free energies.

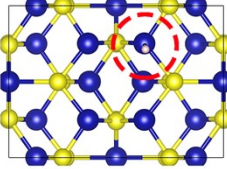
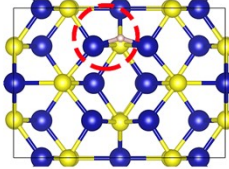
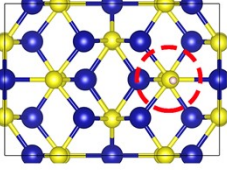
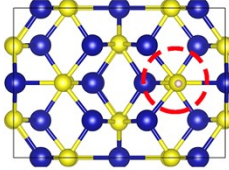
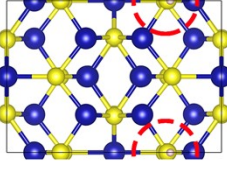
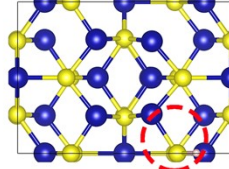
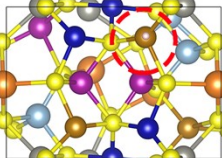
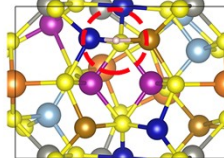
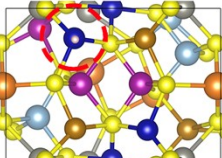
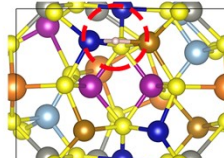
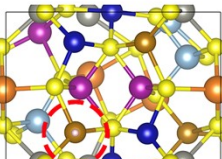
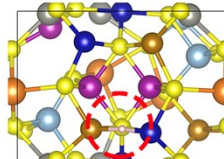
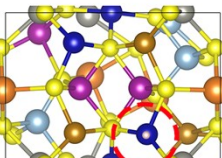
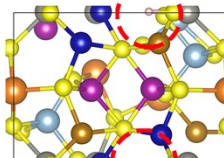
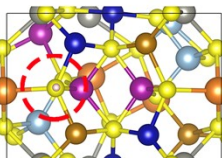
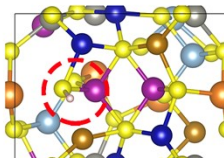
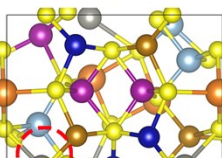
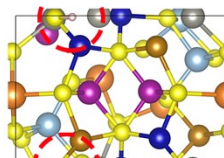
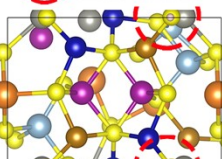
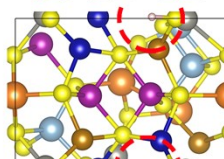
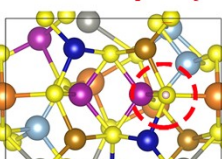
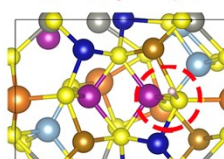
adsorption sites	placed sites	stabilized sites	ΔG (eV)
Co_9S_8 -H1			-0.34
Co_9S_8 -H2			1.06
Co_9S_8 -H3			0.68

Table. S4 Statistical table of $(\text{ZnCoMnFeAlMg})_9\text{S}_8$ adsorption sites and corresponding Gibbs free energies.

adsorption sites	placed sites	stabilized sites	ΔG (eV)
HES-H1			-0.08
HES-H2			0.30
HES-H3			0.04
HES-H4			0.02
HES-H5			0.82
HES-H6			0.72
HES-H7			-0.79
HES-H8			1.45